International Journal of River Basin Management

ISSN: (Print) (Online) Journal homepage: https://www.tandfonline.com/loi/trbm20

An innovative hydrological model for the sparsely-gauged Essequibo River basin, northern Amazonia

Daryl Hughes, Steve Birkinshaw, Geoff Parkin, C. Isabella Bovolo, Brighid Ó Dochartaigh, Alan MacDonald, Angela L. Franklin, Garvin Cummings & Ryan Pereira

To cite this article: Daryl Hughes, Steve Birkinshaw, Geoff Parkin, C. Isabella Bovolo, Brighid Ó Dochartaigh, Alan MacDonald, Angela L. Franklin, Garvin Cummings & Ryan Pereira (14 Nov 2023): An innovative hydrological model for the sparsely-gauged Essequibo River basin, northern Amazonia, International Journal of River Basin Management, DOI: 10.1080/15715124.2023.2278678

To link to this article: https://doi.org/10.1080/15715124.2023.2278678

INTERNATIONAL JOURNAL OF RIVER BASIN MANAGEMENT
https://doi.org/10.1080/15715124.2023.2278678

Taylor & Francis
Taylor & Francis Group

RESEARCH ARTICLE

OPEN ACCESS Check for updates

An innovative hydrological model for the sparsely-gauged Essequibo River basin, northern Amazonia

Daryl Hughes [a], Steve Birkinshaw[b], Geoff Parkin[b], C. Isabella Bovolo[c], Brighid Ó Dochartaigh[d], Alan MacDonald[d], Angela L. Franklin[e], Garvin Cummings[f] and Ryan Pereira[a]

[a]The Lyell Centre, Heriot-Watt University, Edinburgh, United Kingdom; [b]School of Engineering, Newcastle University, Newcastle upon Tyne, United Kingdom; [c]Department of Geography, Durham University, Durham, United Kingdom; [d]British Geological Survey, The Lyell Centre, Edinburgh, United Kingdom; [e]Guyana Water Incorporated, Georgetown, Guyana; [f]Guyana Hydrometeorological Service, Georgetown, Guyana

ABSTRACT

Tropical river basins – crucial components of global water and carbon cycles – are threatened by logging, mining, agricultural conversion, and climate change. Thus, decision-makers require hydrological impact assessments to sustainably manage threatened basins, such as the ~68,000 km^2 Essequibo River basin in Guyana. Emerging global data products offer the potential to better understand sparsely-gauged basins. We combined new global meteorological and soils data with established *in situ* observations to build the first physically-based spatially-distributed hydrological model of the Essequibo. We developed new, open source, methods to translate global data (ERA5-Land, WFDE5, MSWEP, and IMERG) into a grid-based SHETRAN model. Comparing the performance of several global and local precipitation and evaporation datasets showed that WFDE5 precipitation, combined with ERA5-Land evaporation, yielded the best daily discharge simulations from 2000 to 2009, with close water balances (PBIAS = −3%) and good discharge peaks (NSE = 0.65). Finally, we tested model sensitivity to key parameters to show the importance of actual to potential evapotranspiration ratios, Strickler runoff coefficients, and subsurface saturated hydraulic conductivities. Our data translation methods can now be used to drive hydrological models nearly anywhere in the world, fostering the sustainable management of the Earth's sparsely-gauged river basins.

ARTICLE HISTORY
Received 25 June 2023
Accepted 30 October 2023

ASSOCIATE EDITOR
Michael Nones

KEYWORDS
Tropical; Guiana Shield; physically-based model; remote-sensing; reanalysis

1. Introduction

Tropical rivers contribute ~67% of global freshwater outflows to the oceans (Huang *et al.* 2012), while tropical forests store around 246 billion tonnes of carbon (Saatchi *et al.* 2011). However, tropical water resources and carbon fluxes are under pressure from changing land use and climate (Regnier *et al.* 2013, Berhe *et al.* 2018). Agriculture drove 6.4–8.8 Mha per year tropical deforestation from 2011 to 2015 (Pendrill *et al.* 2022), industrial mining in tropical forests is expanding (Giljum *et al.* 2022), and climatic changes are affecting the frequency and magnitude of hydrological extremes, impacting fire regimes and potentially causing ecosystem shifts (Armenteras *et al.* 2021). Tropical hydrological research has been hampered by sparse monitoring and inaccurate data (Sheffield *et al.* 2018), owing to inaccessibility and poor infrastructure. Recently, however, the proliferation of global geospatial and hydro-meteorological data from remote-sensing and reanalysis has enabled hydrological impact studies in sparsely-gauged tropical regions including West Africa (Dembélé *et al.* 2020) and Central Africa (Nkiaka *et al.* 2022).

1.1. Research gap

The Essequibo-Mazaruni-Cuyuni River basin is South America's sixth largest river by discharge (Meybeck and Ragu 2012). It plays a crucial role in continental moisture transport (Bovolo *et al.* 2018), and transports high concentrations of solutes to the Atlantic Ocean (Raymond and Spencer 2015). Parts of the basin are threatened by deforestation, mining, agriculture and pollution (Government of Guyana 2016, Department of Environment 2019), and some tributaries (e.g. Amaila River Falls) are earmarked for hydropower development. Although there is an urgent need to assess the potential impact of such changes, limited modelling has been done. Global hydrological models (GHMs) (e.g. Ward *et al.* 2014, Stacke and Hagemann 2021) have been run on large grid cells (typically 1°), with surface water drainage derived from coarse (e.g. 0.5°) Digital Elevation Models (DEMs) (Telteu *et al.* 2021). Furthermore, they have not used the regionally-accurate forcing data required to simulate streamflow adequately in Amazonia (Getirana *et al.* 2012, Towner *et al.* 2019, Krysanova *et al.* 2020). Moreover, remote-sensing and reanalysis products have severely underestimated rainfall in the central Essequibo basin (Pereira *et al.* 2014a). There is, therefore, an urgent need for an effective purpose-built hydrological model of the Essequibo River basin.

In this study we assessed the suitability of different spatial and atmospheric data for modelling the Essequibo's hydrology, built the first physically-based spatially-distributed (PBSD) hydrological model of the basin, and assessed its suitability for predicting water balances and peak discharges.

CONTACT Daryl Hughes D.Hughes@hw.ac.uk The Lyell Centre, Heriot-Watt University, Edinburgh EH14 4AP, United Kingdom
Supplemental data for this article can be accessed online at https://doi.org/10.1080/15715124.2023.2278678.

2. Data and methods

2.1. Study area

The 154,860 km^2 Essequibo-Mazaruni-Cuyuni basin sits within the Guiana Shield in the Amazonia region (Figure 1). The Essequibo and Cuyuni Rivers, running through Guyana, meet the Mazaruni River stemming from Venezuela at Bartica, before flowing to the Atlantic Ocean. This study focuses on the Essequibo sub-basin to Plantain Island (Lehner and Grill 2013). The sub-basin covers some 68,279 km^2, although the watershed shared with the Takutu River (Amazon basin) moves during the wet season in the 3,500 km^2 Rupununi Portal wetlands (de Souza *et al.* 2020, WWF 2020). The Kanuka and Pakaraima Mountains delineate the western watershed. The northern basin's coastal climate has two wet seasons (May to July; Dec to Jan), while the southern basin's more continental climate has one (May to Aug) (Pereira *et al.*, 2014a). Precipitation is driven by the movement of the Inter-Tropical Convergence Zone (ITCZ) seasonally, and also the El Niño Southern Oscillation (ENSO) (Bovolo *et al.* 2012). Only two large rivers have near continuous long-term discharge records, from January 1950 (Bovolo *et al.* 2009): (1) the Essequibo River at Plantain Island (PI) (2,604 m^3 s^{-1} or 71 km^3 yr^{-1} mean discharge); (2) Potaro River near Kaieteur Falls (KF) (214 m^3 s^{-1} or 7 km^3 yr^{-1}) (HydroMet 2009).

2.2. Model rationale and development approach

We needed a model to represent basin-scale water dynamics and balances, and make robust predictions about the impacts of land cover and climatic changes on future discharges peaks, which drive carbon and nutrient fluxes. PBSD models can provide robust predictions under non-stationary conditions, allowing detailed scenarios to be simulated. PBSD models are needed to understand the impacts of interacting changes in land cover and climate (Ebodé 2022). SHETRAN is a PBSD catchment hydrological modelling package that simulates surface and subsurface flows on a 3D spatial grid (Ewen *et al.* 2000). SHETRAN has been used for impact studies in numerous geographical contexts (e.g. Birkinshaw and Ewen 2000, de Hipt *et al.* 2017, Sreedevi and Eldho 2021). A SHETRAN (v4.5) computational model was built for the Essequibo basin to Plantain Island, where there was a discharge gauge available for model validation. However, the spatial data domain covered the entire Essequibo-Mazaruni-Cuyuni basin (1.1° South to 8.2° North, −62.9° West to −57.7° East) to facilitate future model expansion into the ungauged basin. A 5 km grid resolution was chosen to capture major river channels, while aligning with the coarse resolution of available spatial data and minimising computational demands. The period from 2000 to 2009 was chosen to correspond to available gauge precipitation and discharge data.

The model development approach was as follows: Spatial data selection and processing (Section 2.3); selection and processing of meteorological forcing data (Section 2.4) to create a 'prototype' model with estimated initial parameters; performance assessment to identify the 'most suitable forcings model' (Section 2.5), and; sensitivity analysis of key spatial parameters (Section 2.6).

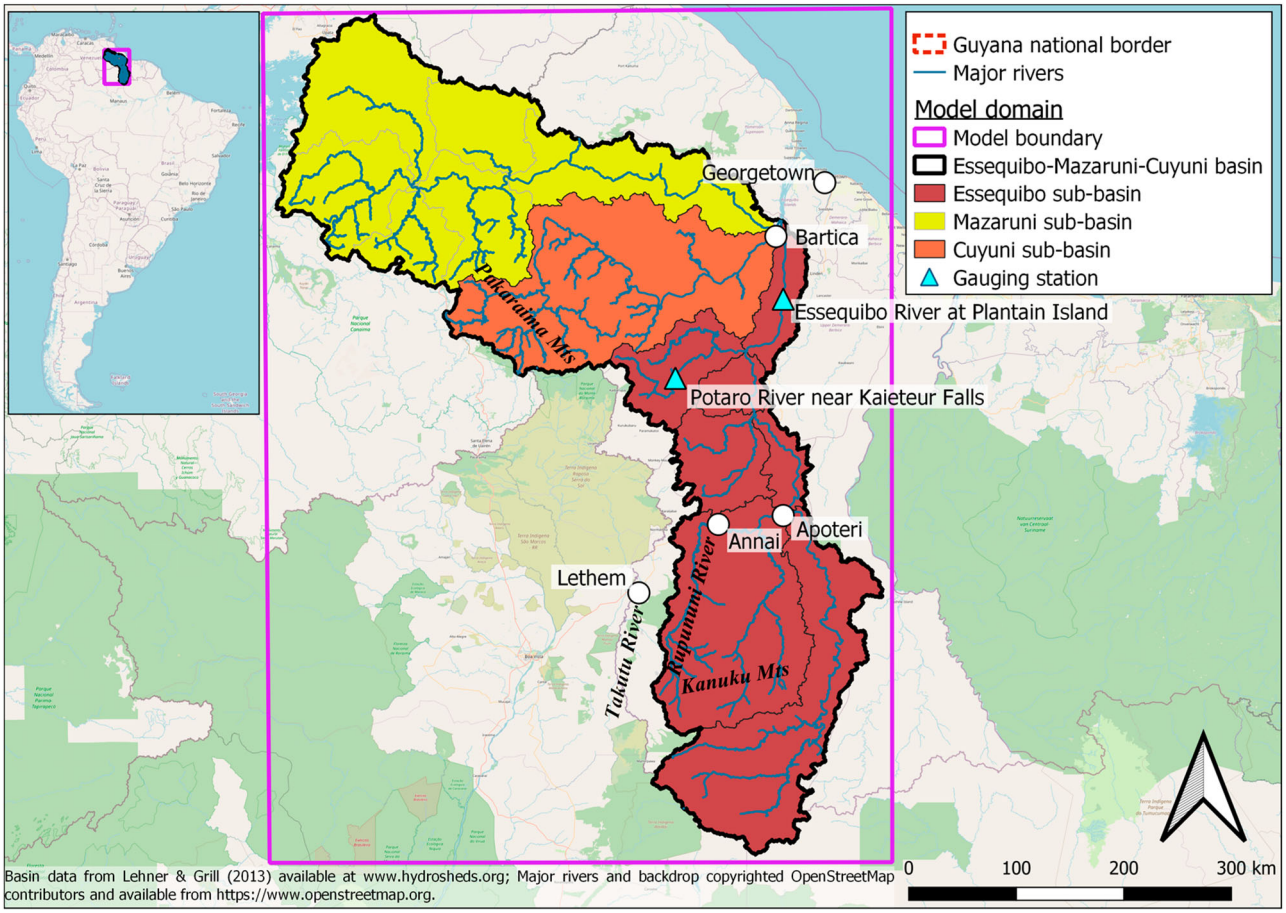

Figure 1. Location of Essequibo River basin in South America.

2.3. Spatial data selection and processing

SHETRAN models are based on DEMs and parameterised using spatial data to describe subsurface hydraulics and land cover properties. The criteria for data selection were determined *a priori* (Table 1). Where multiple potential datasets were available, the most suitable was determined through further testing. For example, DEMs were tested against other hydrographic products. The MERIT-Hydro Adjusted Elevation (Yamazaki *et al.* 2017) river channels and watershed boundary we derived corresponded well to two independent datasets; HydroBASINS (Lehner and Grill 2013) and major river channel locations (OpenStreetMap 2017). Watersheds derived using other products extended erroneously into neighbouring river basins. There was only one soils dataset that included all Maulem-van Genuchten parameters (Montzka *et al.* 2017). Sentinel-2 10 m Land Use/Land Cover (Karra *et al.* 2021) was selected since it has a high resolution and is updated annually.

Key processing steps are detailed in Supplementary Material and briefly described here. The MERIT-Hydro Adjusted Elevation DEM was sink-filled and aggregated to obtain mean and minimum elevations at 5 km resolution. SHETRAN's channel algorithm was applied to minimum elevations to generate a river network (Birkinshaw 2010). A 10 m deep channel was burned in using a River layer (OpenStreetMap 2017). This ensured that the river locations were accurate, especially in flat forested areas, in contrast to many GHMs. Sinks were manually filled near Annai to ensure the Rupununi River converged with the Essequibo River at Apoteri. Sentinel-2 Land Cover (2021–2022) was aggregated to 5 km using nearest neighbour. The 12 Sentinel-2 Land Cover Classes were reclassified into 3 dominant SHETRAN classes: Tropical Forest (342,125 km^2), Grass-Arable (87,975 km^2), and Urban (275 km^2).

PBSD models rely on representative grid-scale parameter values, which may vary considerably within and between grid cells. Vegetation parameters were added from the SHETRAN Manual (Birkinshaw 2021). Soils were parameterised by resampling, to 5 km, the 0.25° (~28 km) Soil-Grids-Schaap parameters for the upper 2 m (Supplementary Material, Research Data). Geology was conceptualised based on lithological maps, descriptions, and geological field reports by the authors (US Army Corps of Engineers 1998, Department of Environment 2019), since full Maulem-van Genuchten parameters were unavailable. In lieu of high resolution hydrostratigraphy, the model assumes a 5 m thick layer of sand and laterite, underlain by 150 m of low permeability bedrock (pers comms Ó Dochartaigh, 2022). Saturated hydraulic conductivity (K) values are based on pumping tests in analogue horizons in Nigeria, which share similar geology and climate (Bonsor *et al.* 2014). The processed data was used to construct a 'prototype' model using initial parameter estimates (Figure 2).

2.4. Meteorological forcing data selection and processing

PBSD hydrological models require meteorological forcing data, e.g. precipitation (P) and evapotranspiration (ET). We needed to force the model with historic data to test it against observed river discharges. The suitability criteria were determined *a priori* (Table 2). Products also needed to be low-cost, available to download, and well- documented. Observed P data was selected from the Guyana Hydrometeorological Service (HydroMet) 147-gauge network (Bovolo *et al.* 2009). Since incomplete records were available for most of the gauges, the eight gauges with the most continuous records (>69% of daily data from 2000 to 2010) were selected and used to create the 8-Rain-Gauges forcing data with Thiessen polygons (Supplementary Material).

To overcome the sparsity of gauge data, the use of global gridded atmospheric products was investigated. Over 30 global P datasets were available, including gauge-based, satellite-related and reanalysis products (Sun *et al.* 2018). Four datasets were selected, based on their suitability for

Table 1. Spatial data criteria and suitability in the Essequibo basin.

Dataset required	Suitability criteria (geospatial and parameters)	Dataset description	Dataset suitability
Digital elevation model (DEM)	Resolution min. 5 km	*MERIT-Hydro Adjusted Elevation (Yamazaki *et al.* 2017)	*Suitable. Corresponds well to HydroBASINS and major river channels
	Topography sufficiently accurate to generate basin area matching HydroBASINS and major river channel locations	MERIT-DEM (90 m) (ibid)	Corresponds poorly
		ALOS World 3D (30 m) (Japan Aerospace Exploration Agency 2021)	Corresponds poorly
Geology	Resolution min. 100 km	BDTICM_M_1 km Depth to Bedrock (Shangguan *et al.* 2017)	Unsuitable. Provides depth estimates only
	Layer depth indication	GLiMv1.0 (Hartmann and Moosdorf 2012)	Unsuitable. Provides no hydraulic properties
	Saturated Water Content (θSat)	GLHYMPS v1.0 (Gleeson *et al.* 2014)	Unsuitable. Provides permeability (k) only
	Residual Water Content (θRes)	GLHYMPS 2.0 (Huscroft *et al.* 2018)	Unsuitable. Provides permeability (k) only
	Saturated Conductivity (K)		
	vanGenuchten- alpha (vGα)		
	vanGenuchten-n (vGn)		
Soil	As for Geology	* Hydraulic-Params Soil-Grids-Schaap (0.25°) (Montzka *et al.* 2017)	*Suitable. Parameter values are physically plausible
		Harmonized World Soil Database v 1.2 (Wieder *et al.* 2014)	Contains soil texture only
Land cover	Resolution min. 5 km	*Sentinel-2 10 m Land Use/Land Cover (Karra *et al.* 2021)	*Suitable. High accuracy and annual product release
	Broad land cover types, e.g. forest, short vegetation, urban	Copernicus Global Land Service: Land Cover 100 m (Buchhorn *et al.* 2020)	Suitable
	Strickler coefficient (Str)	Land Cover Map (GLC2000 – JRC)	Suitable
	Actual to Potential Evapotranspiration ratio (AE:PE)	ESA WorldCover (ESA 2017)	Suitable
	Canopy storage capacity (CSC)		

Note: *Indicates most suitable dataset.

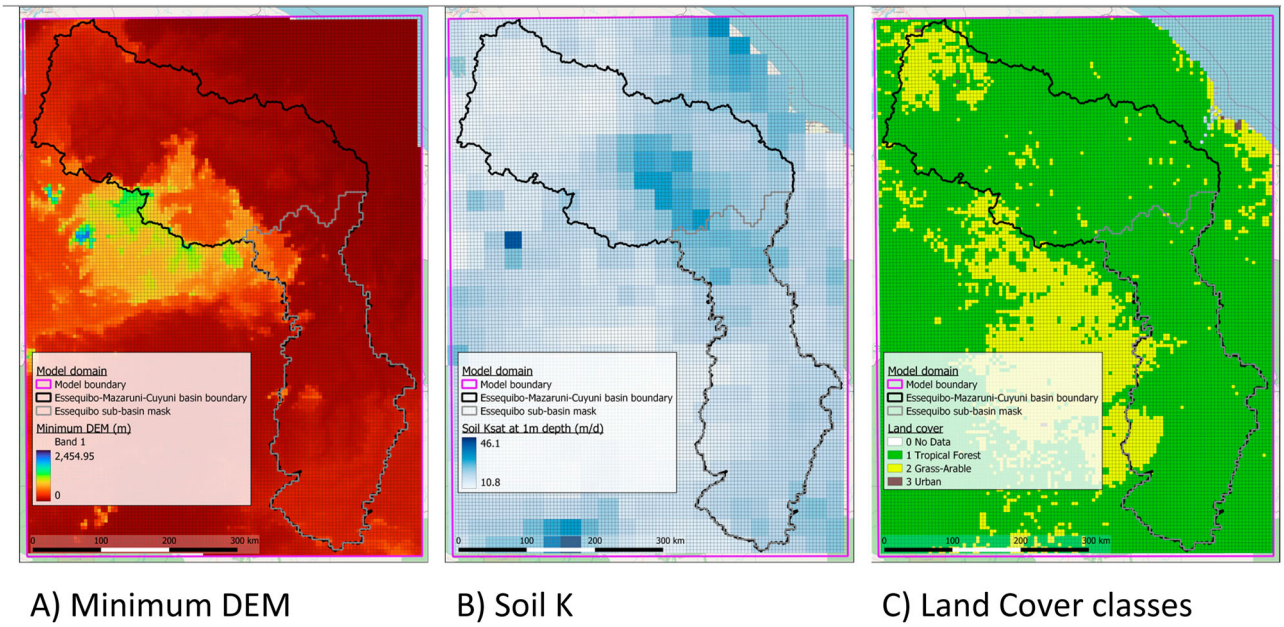

Figure 2. Key spatial data used in Essequibo model. (A) Minimum DEM (Source: MERIT-Hydro Adjusted Elevation (Yamazaki *et al.* 2017)); (B) Soil (Source: Hydraulic-Params Soil-Grids-Schaap (0.25°) (Montzka *et al.* 2017)); (C) Land Cover. Source: Sentinel-2 10 m Land Use/Land Cover (Karra *et al.* 2021).

Table 2. Requirements and suitable precipitation and evapotranspiration for the Essequibo-Mazaruni-Cuyuni data domain.

Variable	Dataset name	Variable name	Highest spatial resolution (Min. 1° × 1°, ~90 km)	Highest time resolution (Min. 1-day)	Time period (2000 –2009)	Data source	Key ref
P	8-Rain-Gauges	-	-	1-day	2000–2010	Rain gauges	(Bovolo *et al.* 2009)
P	ERA5-Land	'tp' (total precipitation)	0.1° × 0.1°	1-hour	1950–present	Reanalysis	(Muñoz Sabater 2019)
P	WFDE5 v2.1	'Rainf' (rainfall flux)	0.5° × 0.5°	1-hour	1979–2019	Reanalysis	(Cucchi *et al.* 2022)
P	MSWEP v2.8	'precipitation'	0.1° × 0.1°	3-hour	1979–present	Gauge, satellite, reanalysis	(Beck *et al.* 2019)
P	IMERG v6.0	'pr' (precipitation)	0.1° × 0.1° (0.5° × 0.5° used)	30-minute	2000–present	Satellite	(Huffman *et al.* 2018)
ET	Kaieteur Pan	-	-	Seasonal	2005–2007	Evaporation pan	-
ET	ERA5-Land	'total evaporation'	0.1° × 0.1°	1-hour	1950–present	Reanalysis	(Muñoz Sabater 2019)

hydrological modelling and data availability: ERA5-Land, WFDE5, MSWEP, and IMERG. ERA5-Land (ECMWF Reanalysis v5) is part of the ERA5 product family, at higher spatial resolution. ERA5 assimilates more gauge-satellite data than its predecessor ERA-Interim (Muñoz-Sabater *et al.* 2021). Its 'total precipitation' variable is an input forcing of ERA5-Land. ERA5 has been widely used in land surface and hydrological models. Although it tends to have a wet bias in the tropics, it has a 10–20% dry bias over most of the Essequibo (compared to GPSC-SG) (Hassler and Lauer 2021), and underestimates daily rainfall by 1.5–4 mm over the Guiana Shield (compared to TRMM) (Hersbach *et al.* 2020). WFDE5 (WATCH Forcing Data methodology applied to ERA5) provides bias-corrected ERA5 variables, including precipitation, to improve hydrological modelling (Cucchi *et al.* 2020). MSWEP 2 (Multi-Source Weighted-Ensemble Precipitation) merges gauge, satellite, and reanalysis products (Beck *et al.* 2019) to provide reliable global P estimates. MSWEP products have been used widely, including to study hydrological extremes in the Amazon River basin (Wongchuig *et al.* 2019). IMERG 6 (Integrated Multi-satellitE Retrievals for GPM) intercalibrates and merges P data from many satellites from 2000 to present (Huffman *et al.* 2018). It has been successfully used for hydrological modelling in Amazonia (Satgé *et al.* 2021).

ERA5-Land, WFDE5 and IMERG 6 were downloaded from the Copernicus Climate Data Store (Muñoz Sabater 2019, Huffman *et al.* 2020, Cucchi *et al.* 2022). MSWEP 2 was batch downloaded using Rclone (GloH20 2022). Each dataset required translation into SHETRAN input files. Bespoke methods using Python 3 and QGIS were developed to extract target variables, clip to domain, align to model grid, aggregate to daily time step, and re-dimension from 3D to 2D. Workflows and codes for translating WFDE5 precipitation and ERA5-Land ET have been made freely-available (Supplementary Material; Research Data).

Some consistent and plausible point-source ET data was available from a weather station at Kaieteur Falls, an upland forest area. Pan evaporation data from January 2005 to December 2007 was used to derive 'Kaieteur Pan' seasonal ET estimates (Supplementary Material). However, this data was not spatially distributed. Many spatially-distributed ET products were available, from remote-sensing, reanalysis, and hydrological model outputs (Mohan *et al.* 2020, Senay *et al.* 2020, Schneider and Hogue 2022, Zhu *et al.* 2022).

Hydrological impact studies in sparsely-gauged areas have demonstrated that gridded ET suitability depends on study purpose and regional climate (Ansari *et al.* 2022, Wang *et al.* 2022). In the Amazon River basin, several products provide reasonable estimates of annual magnitude, but may overestimate monthly variability and exhibit divergent multi-year trends (Wu *et al.* 2020). The ERA-5 Land (ECMWF Reanalysis v5) gridded dataset was selected. This includes several ET variables, of which 'total evaporation' was used since it most closely matched pan evaporation at Kaieteur Falls and Lethem. Other ET products did not meet the specified spatial and temporal resolution.

2.5. Model performance assessment

The model was spun up from 1 January 2000, and assessed from 1 January 2001 to 1 December 2008 (7 years, 11 months) to match the observed discharge data. Model performance was assessed using river discharge at Plantain Island (PI) and Kaieteur Falls (KF) (Figure 1). No further variables (e.g. soil moisture and groundwater level) were available for multi-objective validation (Gupta *et al.* 1998). Four objective functions were calculated for daily values, with missing days excluded: (1) Percentage bias (PBIAS), where lower values are better, with positive values indicating overprediction and *vice versa*; (2) Root Mean Squared Error (RMSE), where lower values are better; (3) Nash-Sutcliffe Efficiency (NSE), where a value of zero indicates performance equivalent to the mean and one indicates a perfect fit, and; (4) Kling-Gupta Efficiency (KGE) where a value of −0.41 indicates performance equivalent to the mean and one indicates a perfect fit (Gupta *et al.* 2009, Moriasi *et al.* 2015, Knoben *et al.* 2019). The model required low PBIAS (e.g.< ± 20%) to predict water balances, and 'good' NSE (e.g. >0.6) to reproduce peak discharges.

2.6. Spatial parameter sensitivity analyses

The 'most suitable forcings model' contained initial soil and vegetation parameter values within a plausible range (Table S3, Supplementary Material). Single-factor sensitivity analyses were performed on parameters critical to SHETRAN (de Hipt *et al.* 2017, Sreedevi *et al.* 2019), i.e. Actual to Potential Evapotranspiration ratio (AE:PE) at field capacity; Canopy Storage Capacity (CSC); Strickler overland flow of Land (Str_{Land}) and Channels ($Str_{Channel}$); and the Saturated Hydraulic Conductivity of Soil (K_{Soil}) and Sand-Laterite ($K_{Sand\text{-}Laterite}$) (Table 3). Each parameter was changed by up to ±30% and −80 to + 400%, depending on its range of variability (Research Data – Essequibo Model Simulation Results). For instance, Stricker values of Grass-Arable may range from 5 to 10 (Engman 1986). Meanwhile, values of $K_{Sand\text{-}Laterite}$ may range locally from 0.5 to 400 m d^{-1}, although during pumping tests they are typically in the range of 5–50 m d^{-1} (Bonsor *et al.* 2014). Sensitivity was assessed using objective functions (QMAX, PBIAS, NSE, KGE) for river discharge at PI and KF. Given the gauge sparsity, model calibration could pose a substantial risk of overfitting, leading to overconfidence in model outputs and reduction in predictive ability under non-stationary conditions (Yang *et al.* 2022). The 'blind validation' approach was therefore deployed to prevent overfitting (Parkin *et al.* 1996).

Table 3. Initial parameter values in prototype model, with relative changes during sensitivity testing (Full results in Research Data – Essequibo Model Simulation Results).

Parameter	Spatial distribution	Initial value	Relative change
AE:PE	Tropical-Forest	1.0 (-)	± 10%, 20%, 30%
AE:PE	Grass-Arable	0.6 (-)	± 10%, 20%, 30%
CSC	Tropical-Forest	5 (mm)	± 10%, 20%, 30%
CSC	Grass-Arable	1.5 (mm)	± 10%, 20%, 30%
Str_{Land}	Tropical-Forest	1 (-)	± 10%, 20%, 30%
Str_{Land}	Grass-Arable	5 (-)	± 10%, 20%, 30%
$Str_{Channel}$	All river channels	20 (-)	± 10%, 20%, 30%
K_{Soil}	All grids, 0–2 m depth	0.013 m d^{-1} (min) 0.018 m d^{-1} (mean) 0.021 m d^{-1} (max)	± 20%, 50%, 80%
$K_{Sand\text{-}Laterite}$	All grids, 2–7 m depth	20 m d^{-1}	± 20%, 50%, 80%

3. Results

3.1. Model performance assessment

The prototype model was run with the five P and two ET products ($N = 10$) and assessed at the downstream PI and upstream KF stations.

3.1.1. Prototype performance with Kaieteur pan evaporation data

With Kaieteur Pan ET (rows 1–5, Table 4), the model generally performed better at PI than KF. Being further downstream, PI allowed for greater compensation of discharge errors, i.e. over- and under-prediction of discharges in upstream tributaries mutually cancelled as they propagate downstream. WFDE5 P performed best at PI, generating the lowest PBIAS (−25%), a moderate NSE (0.68) and KGE = 0.72. Furthermore, WFDE5 was the only P data that performed well at KF. This demonstrates the value of bias-corrected P data for impact studies (Cucchi *et al.* 2020). ERA5-Land, MSWEP and IMERG precipitation all performed moderately at PI, suffering from negative PBIAS (−53% to −59%), low NSE (0.25–0.41), and KGE 0.33–0.42. All three performed worse at KF, with severe negative biases (−78% to −80%) resulting in negative NSE and KGE. All three were outperformed by the less sophisticated 8-Rain-Gauges (Thiessen polygons) data, perhaps because it accurately recorded local rainfall dynamics. Overall, WFDE5 was the best performing dataset across all metrics at both PI and KF.

3.1.2. Prototype performance with ERA5-Land total evaporation data

With ERA5-Land ET (rows 6–10, Table 4), the models performed better due to more accurate water balances. Once again, the WFDE5 forcing performed best overall at PI (Figure 3), generating low PBIAS (−3%), moderate NSE (0.65) and KGE = 0.74, although NSE decreased slightly (from 0.68 to 0.65), because it overestimated wet season high peak discharges (Figure 4), to which NSE is particularly sensitive (Gupta *et al.* 2009). Although ERA5-Land, MSWEP and IMERG performed better at PI, they still suffered from a substantial negative PBIAS (−29% to −36%). Only WFDE5 performed well at KF (Figure 5), with a closely fitted flow duration curve from 0% to 80% exceedance (Figure 6). In contrast, ERA5-Land, MSWEP and IMERG performed poorly at KF, where their very negative PBIAS (−69% to

Table 4. Objective functions for simulated daily discharge at Plantain Island and Kaieteur Falls, with Kaieteur Pan evaporation and ERA5-Land 'total evaporation'.

		Plantain Island				Kaieteur Falls			
P forcing	ET forcing	PBIAS	NSE	RMSE (m^3s^{-1})	KGE	PBIAS	NSE	RMSE (m^3s^{-1})	KGE
ERA5-Land	Kaieteur Pan	−53%	0.41	1612	0.41	−80%	−0.54	224	−0.14
WFDE5	Kaieteur Pan	−25%	0.68	1195	0.72	−12%	0.55	121	0.75
MSWEP	Kaieteur Pan	−59%	0.25	1816	0.33	−78%	−0.56	226	−0.10
IMERG	Kaieteur Pan	−52%	0.35	1691	0.42	−78%	−0.47	219	−0.09
8-Rain-Gauges	Kaieteur Pan	−58%	0.05	2053	0.24	−35%	0.03	178	0.47
ERA5-Land	ERA5-Land	−32%	0.66	1219	0.67	−72%	−0.30	206	−0.02
***WFDE5**	***ERA5-Land**	**−3%**	**0.65**	**1236**	**0.74**	**−3%**	**0.56**	**119**	**0.79**
MSWEP	ERA5-Land	−36%	0.65	1240	0.63	−69%	−0.31	207	0.05
IMERG	ERA5-Land	−29%	0.55	1414	0.66	−71%	−0.24	201	0.04
8-Rain-Gauges	ERA5-Land	−43%	0.33	1711	0.45	−26%	0.09	172	0.54

NB *indicates best overall forcing data combinations.

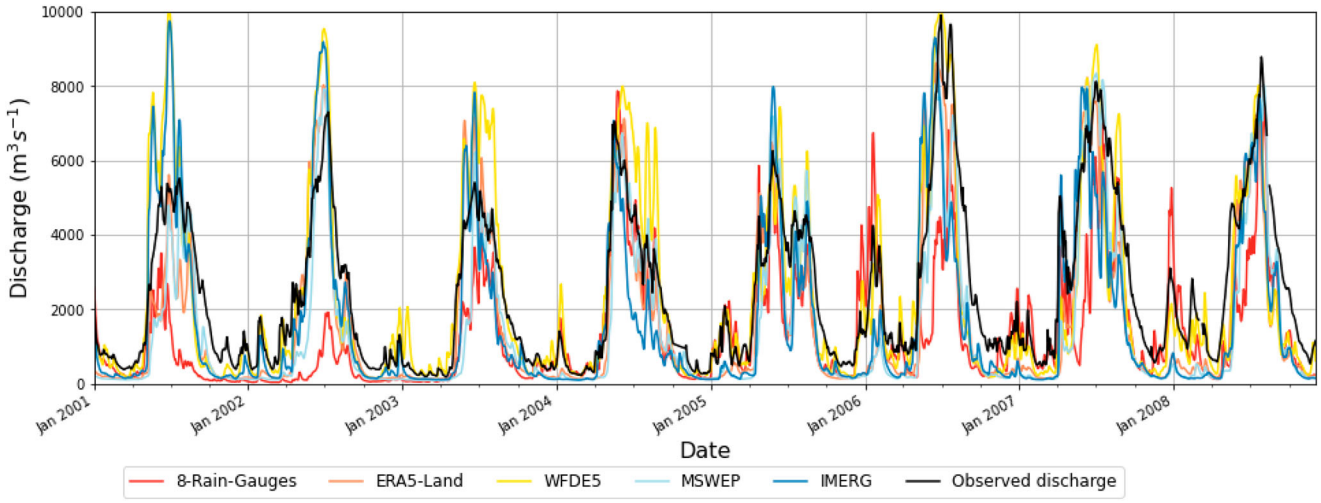

Figure 3. Simulated and observed hydrographs at Plantain Island (downstream), with different precipitation forcings and ERA5-Land ET. January 2001 to December 2008.

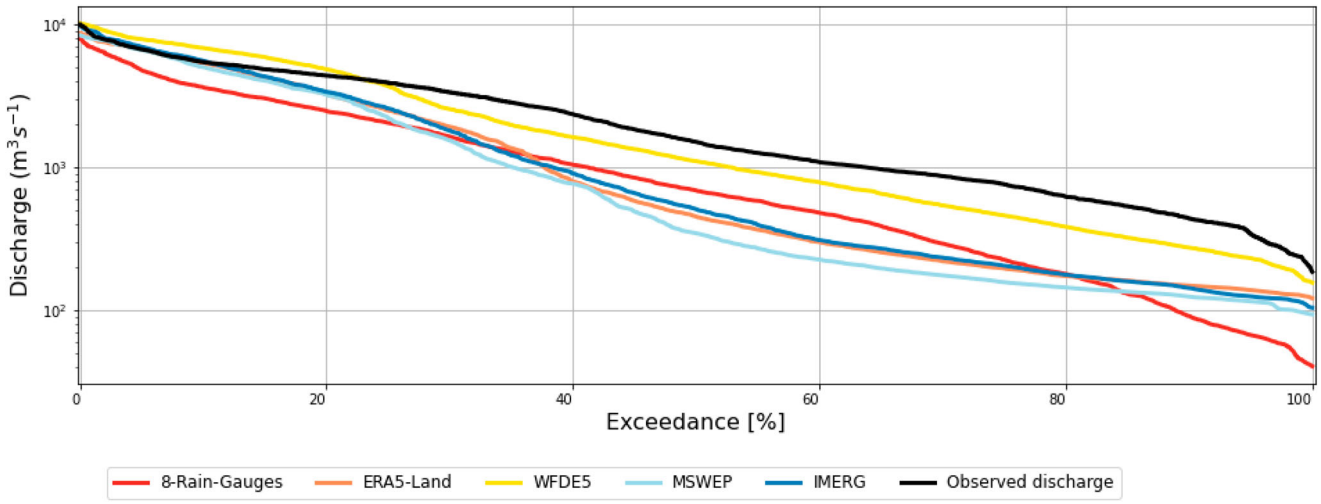

Figure 4. Simulated and observed flow duration curves at Plantain Island (downstream), with different precipitation forcings and ERA5-Land ET. January 2001 to December 2008.

−72%) drove negative NSE and low KGE. All three were outperformed at KF by 8-Rain-Gauges. Overall, WFDE5 performed best across most metrics at PI and KF. In summary, the model was highly sensitive to the forcing data used, performing best with the combination of WFDE5 P and ERA5-Land ET data.

3.2. Spatial parameter sensitivity analyses

The sensitivity analysis demonstrates that, for discharge at PI, the WFDE5 – ERA5-Land model was most sensitive to AE:PE, moderately sensitive to Str_{Land}, $Str_{Channel}$, $K_{Sand\text{-}Laterite}$ and K_{Soil}, and insensitive to CSC (Figure 7,

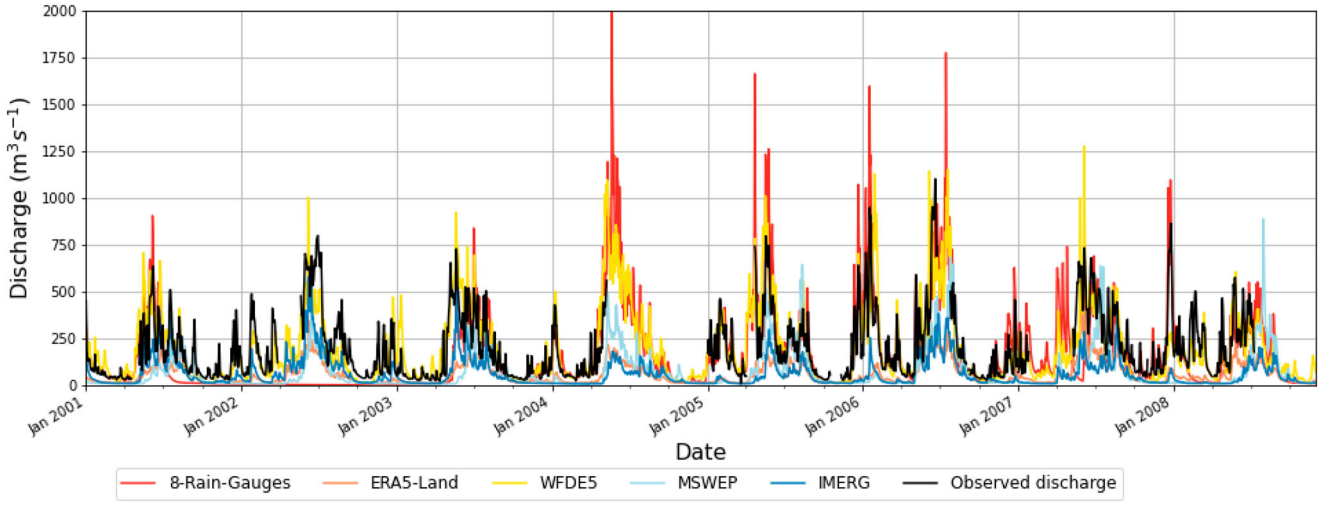

Figure 5. Simulated and observed hydrographs near Kaieteur Falls (upstream), with different precipitation forcings and ERA5-Land ET. January 2001 to December 2008.

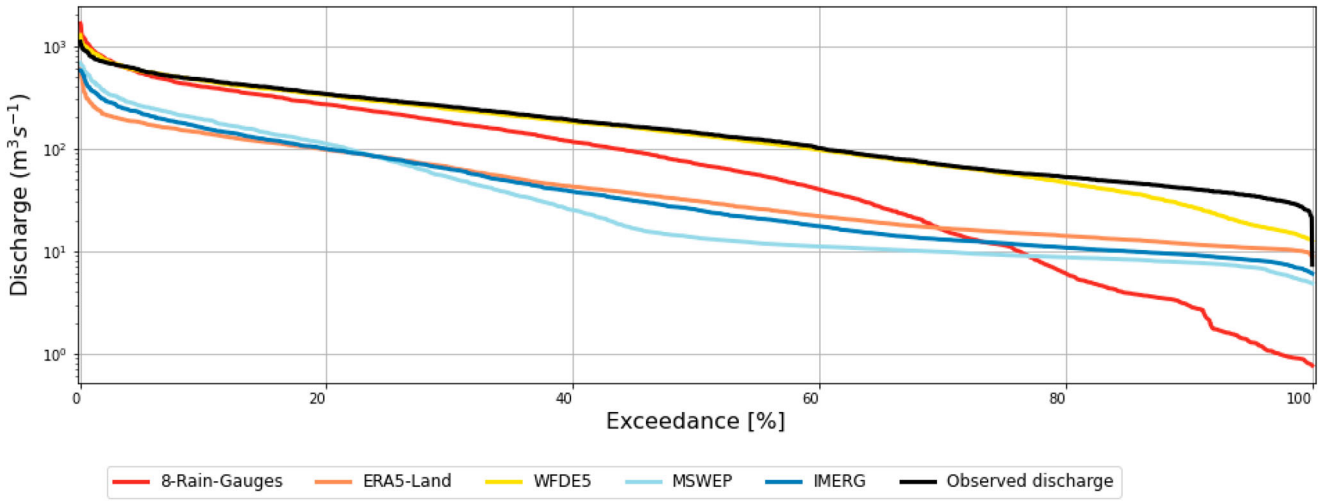

Figure 6. Simulated and observed flow duration curves near Kaieteur Falls (upstream), with different precipitation forcings and ERA5-Land ET. January 2001 to December 2008.

Research Data – Essequibo Model Simulation Results). These findings are broadly similar for KF, although QMAX, NSE and KGE were less sensitive to AE:PE (Figure 8).

At PI, setting AE:PE at −30% resulted in a 6% increase in PBIAS (from −3% to +3%) and corresponding 216 $m^3 s^{-1}$ increase in QMAX, while NSE declined (from 0.65 to 0.60), and KGE declined (from 0.74 to 0.68). Conversely, setting AE:PE at +30% increased NSE and KGE. Setting Str_{Land} at −30% made little difference to PBIAS, although it did decrease QMAX (by 258 $m^3 s^{-1}$), and it increased NSE (by 0.04) and KGE (by 0.03). The effects of modifying $Str_{Channel}$ were similar to Str_{Land}. The model was quite sensitive to $K_{Sand\text{-}Laterite}$; setting this at +100% increased NSE (by 0.02) and KGE (by 0.03). Conversely, reducing $K_{Sand\text{-}Laterite}$ decreased model performance. Changing K_{Soil} had similar effects, although with less sensitivity. In summary, the model was most sensitive to changes in AE:PE, and somewhat sensitive to Strickler and subsurface K. Nevertheless, the model was more sensitive to forcing data than to soil and vegetation parameters.

4. Discussion

This innovative modelling approach takes global forcing data (WFDE5 precipitation and ERA5-Land evaporation) and translates it to a 5 km SHETRAN grid for the Essequibo River basin. Running the WFDE5 – ERA5-Land model for a ten-year daily simulation costs ~4 h of computational time on single core 3.6 GHz CPU with 32 GB RAM. From 2000 to 2009, this reproduces river discharge well, with very good PBIAS (−3%). The shapes of the hydrographs match well at Plantain Island (NSE = 0.65) and Kaieteur Falls (NSE = 0.56). Wet season peaks are generally well reproduced, although the model tends to overestimate their magnitudes and overestimate their recession gradients. Correspondingly, the model tends to underestimate dry season flows. This indicates that the groundwater component requires further development. Nonetheless, the ability to simulate discharge peaks makes it suitable to use the model for estimating flood risk to infrastructure and riverine solute transport (Regnier *et al.* 2013). Indeed, the Essequibo model

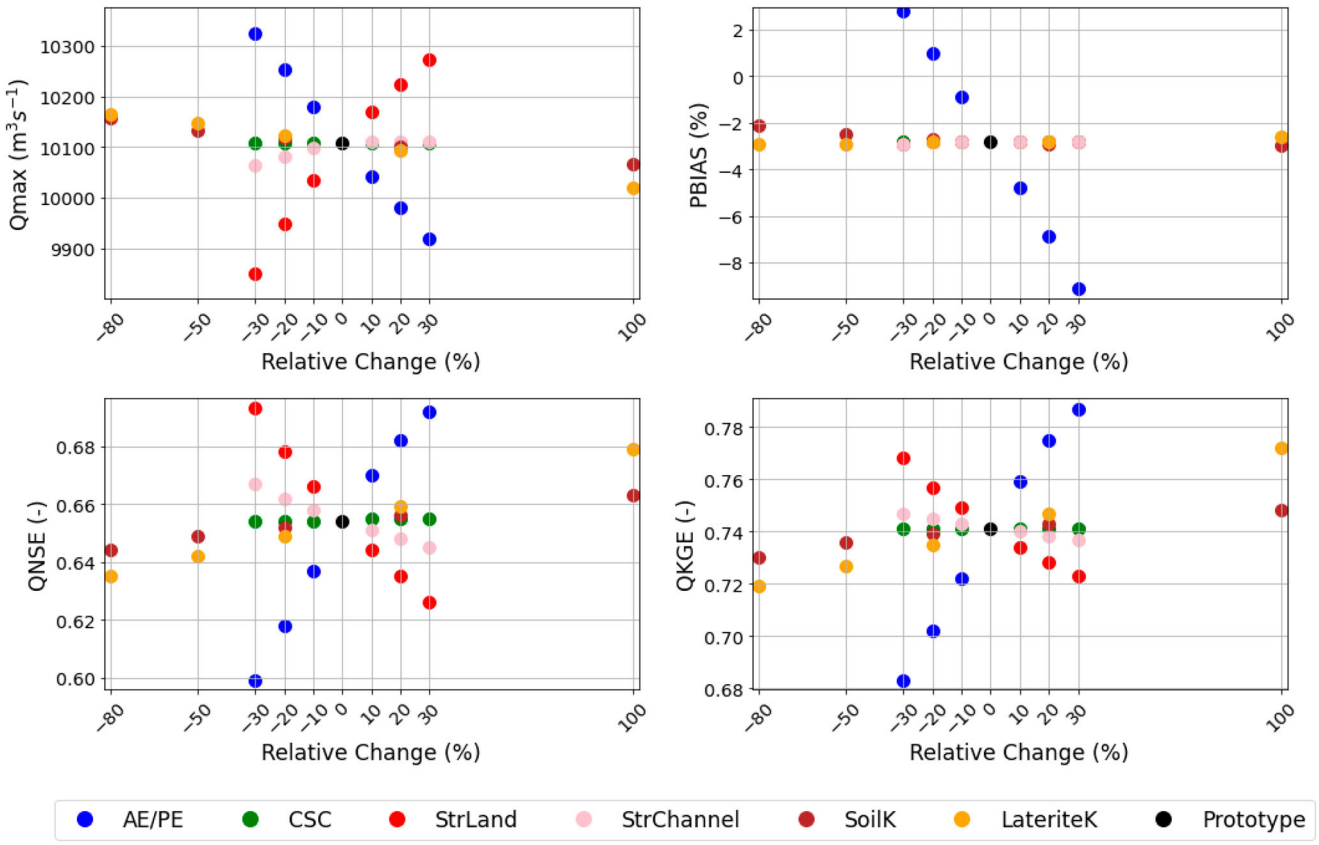

Figure 7. Sensitivity analysis metrics for Essequibo at Plantain Island in ERA5 – WFDE5 model. NB +400% not plotted.

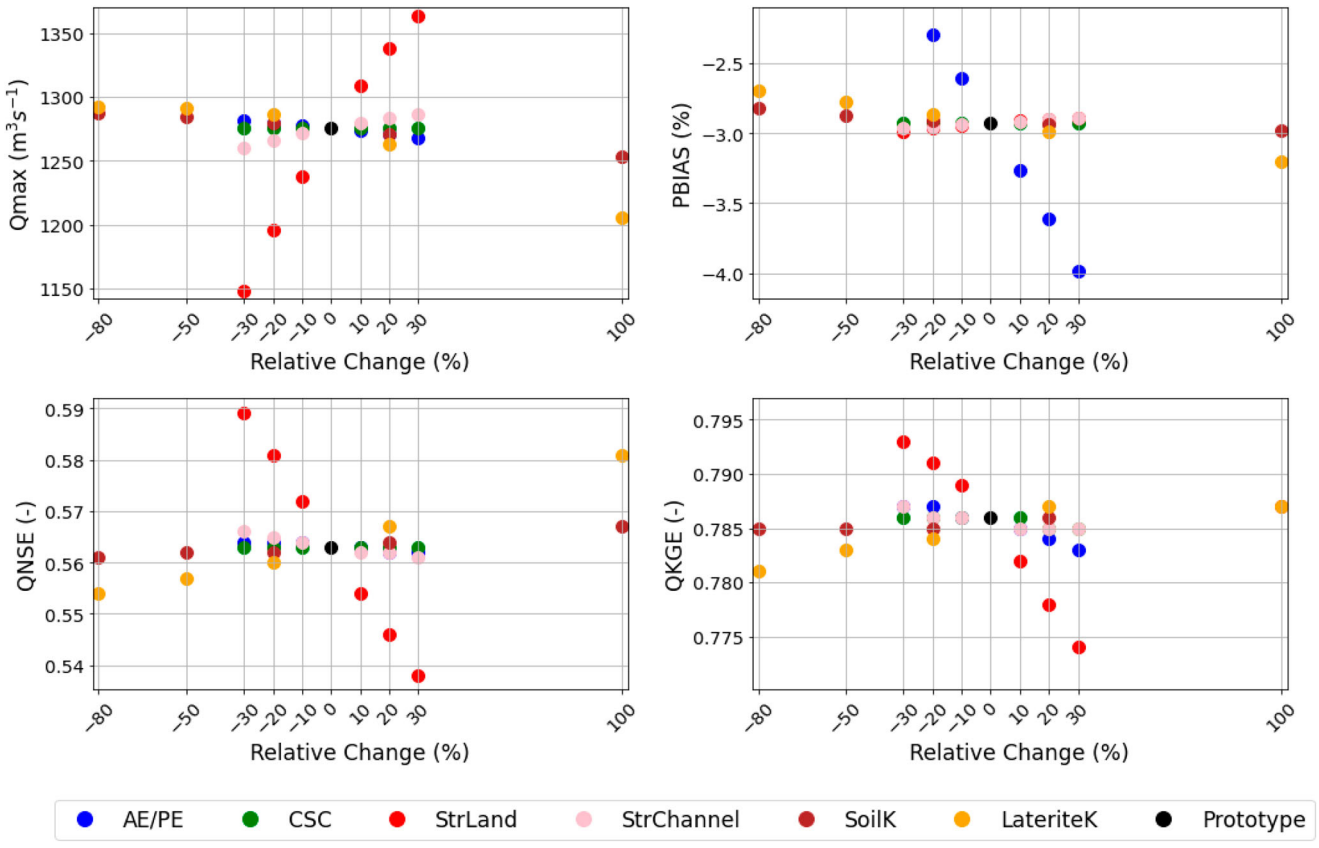

Figure 8. Sensitivity analysis metrics for Essequibo at Kaieteur Falls in ERA5 – WFDE5 model. NB +400% not plotted.

outperforms most GHMs in Amazonia (Getirana *et al.* 2012, Towner *et al.* 2019, Krysanova *et al.* 2020), as judged by the PBIAS and KGE metrics.

PBSD models require high volumes of data to parameterise them well. Our model could be improved by further parameterisation. Firstly, soil hydraulics data could be validated

or modified though *in situ* measurements. Secondly, the broad geological assumptions could be developed further, given that the model is sensitive to subsurface parameters. Improvements in continental-scale geological mapping could be used to refine stratigraphy and hydraulic properties (e.g. MacDonald *et al.* 2012), with performance assessed using *in situ* measurements or remote sensing (Adams *et al.* 2022) to enable multi-objective model assessment. The sensitivity analysis at PI and KF suggests that improved model performance (in terms of PBIAS, NSE and KGE) could be achieved by a combination of slightly decreasing AE:PE, decreasing Str and increasing subsurface K. These factors would likely reduce the overprediction of wet season discharge peaks, and maintain higher baseflows during dry periods (through aquifer discharges into river channels). It would therefore be worthwhile to obtain and incorporate further empirical data. Alternatively, the sensitivity analysis could be used to inform calibration efforts (de Hipt *et al.* 2017). A calibration exercise would need to maintain parameters within plausible limits to mitigate the risk of overfitting, especially given the uncertainty inherent in the forcing products. Given current data limitations, we recommend that future modelling studies incorporate parameter uncertainty by running parameter ensembles.

Global forcing data have enabled PBSD hydrological modelling in the Essequibo River basin, despite the sparsity of hydrometric data. We, therefore, suggest that many previous barriers to using satellite data to improve water resources management have been overcome (Sheffield *et al.* 2018). Nevertheless, the quality of geospatial and atmospheric forcing data ultimately relies on ground-level data for validation. Moreover, high quality, continuous *in situ* hydrometric monitoring would enable more robust predictions in sparsely-gauged river basins, particularly in remote upstream sub-basins. The high overall performance resulting from the bias-corrected WFDE5 dataset, and good local performance from the rain gauge at Kaieteur Falls, indicates the value of improved *in situ* rainfall monitoring, as a complement to remote sensing datasets. Further investment in meteorological and hydrometric monitoring (e.g. eddy covariance flux towers for ET, and river gauging in remote inland locations) would support model developments. Nonetheless, the model can be spatially and temporally refined to facilitate better process representation at the headwater scale, where there is a direct link between terrestrial and aquatic processes (Pereira *et al.*, 2014b). The model forcing timestep could be decreased from 24 to 1 h/s using the WFDE5 and ERA5-Land forcing data. If combined with higher spatial resolution, this could allow catchment responses to sub-daily (e.g. convective) rainfall events to be simulated. Land cover can also be updated annually (Karra *et al.* 2021). Future data releases may allow simulations to be extended to the near present and offer digital twin potential. ERA5-Land (P and ET) latency is currently five days (Muñoz-Sabater *et al.* 2021). However, WFDE5 P is released only periodically (currently to 2019).

Our approach can be adapted for other sparsely-gauged regions. By translating global data into grid-based PBSD models (Supplementary Materials), assessing the suitability of forcing data, and validating against a small volume of *in situ* observations, we can improve upon previous GHMs. Our approach can, thereby, help to answer crucial scientific and engineering questions in sparsely-gauged basins around the world. For instance, what would be the impacts of mining and deforestation on tropical hydrology, especially given the disruption of continental moisture transport (Bovolo *et al.* 2018)? How might global climate changes affect patterns of floods, droughts, and fires? How can policymakers sustainably manage use and water resources (Department of Environment 2019)? Furthermore, how could changing hydrological dynamics alter global solute fluxes (Berhe *et al.* 2018; Pereira *et al.*, 2014b)? By addressing these questions, this modelling approach can guide land use planning, water resources planning, and climate adaptation.

5. Conclusions

This study presents an innovative approach to building PBSD models using global forcing data, and the resulting hydrological model of the sparsely-gauged Essequibo River basin. We identified the most suitable geospatial data available and used this to build a SHETRAN model. We subsequently forced this using gauge data, plus gridded atmospheric data from ERA5-Land, WFDE5, MSWEP, and IMERG. The resulting simulated discharges were highly sensitive to the meteorological forcing data used. The bias-corrected WFDE5 precipitation data, and ERA5-Land total evaporation data yielded the best model performance for predicting hydrological peaks, suggesting these are the most representative data available for the Amazonia region. The model was also somewhat sensitive to geospatial runoff coefficients and subsurface permeability, both of which are difficult to measure across the model domain. The new Essequibo model enables hydrological impact studies of land use and climate change on future water and carbon fluxes to support, e.g. water resources, climate adaptation and land use planning.

This study demonstrates that global datasets can be used to overcome gauge sparsity to build effective spatially-distributed hydrological models in tropical regions. Our approach, including new data translation methods (Supplementary Material), may now be used to build grid-based hydrological models almost anywhere on Earth. In the future, these methods can be updated to harness higher-quality, lower latency meteorological products. This study indicates that synthesising the sometimes disparate endeavours of *in situ* hydrometry, earth observation, and hydrological modelling has great potential to advance environmental science and foster sustainable development.

Acknowledgments

This project was funded by the 'Breathing Oceans: understanding the organic skin that modulates the exchange of greenhouse gases between the atmosphere and the ocean' (BOOGIE) project from the European Research Council under the European Union's Horizon 2020 research and innovation programme (grant number 949495). The model development and input data analyses were based on concepts developed over several years by GP, CIB, RP and Tom Wagner (Lyell Centre). A first (non-working) test model received contributions from Haymawattie Danny and Kelvin Samaroo (both of HydroMet) and Roxroy Bollers (formerly of the Iwokrama International Centre for Rainforest Conservation and Development) whose help is gratefully acknowledged. The meteorological data was kindly provided by HydroMet. Weather stations with reliable data were chosen with the help of Vidayshree Diana Misir (HydroMet). BÓD and AM (also of British Geological Survey) helped conceptualise a simple hydrogeological model with BÓD's field observations of shallow groundwater in the sand aquifer in the

North Rupununi. Beth Cowling (Lyell Centre) user tested the global data translation scripts.

Disclosure statement

No potential conflict of interest was reported by the author(s).

Funding

This work was supported by H2020 European Research Council [grant number 949495].

CRediT statement

Daryl Hughes: Conceptualisation, Methodology, Software, Formal analysis, Investigation, Data curation, Writing – Original Draft, Visualisation.
Steve Birkinshaw: Conceptualisation, Methodology, Software, Writing – Review & Editing.
Geoff Parkin: Conceptualisation, Methodology, Writing – Review & Editing.
Brighid Ó Dochartaigh: Methodology.
Alan MacDonald: Writing - Review & Editing.
C. Isabella Bovolo: Conceptualisation, Methodology, Writing – Review & Editing.
Garvin Cummings: Data curation.
Angela L. Franklin: Writing – Review & Editing.
Ryan Pereira: Conceptualisation, Methodology, Resources, Writing – Review & Editing, Supervision, Project administration, Funding acquisition.

ORCID

Daryl Hughes http://orcid.org/0000-0002-7733-6499

References

Adams, K.H., *et al.*, 2022. Remote sensing of groundwater: current capabilities and future directions. *Water Resources Research*, 58 (10), 1–27.
Ansari, R., Usman Liaqat, M., and Grossi, G., 2022. Evaluation of gridded datasets for terrestrial water budget assessment in the Upper Jhelum River basin-South Asia. *Journal of Hydrology*, 613, 128294.
Armenteras, D., *et al.*, 2021. Fire-induced loss of the world's most biodiverse forests in Latin America. *Science Advances*, 7, 3357–3370. Available from: https://www.science.org
Beck, H.E., *et al.*, 2019. MSWep v2 global 3-hourly 0.1° precipitation: methodology and quantitative assessment. *Bulletin of the American Meteorological Society*, 100 (3), 473–500.
Berhe, A.A., *et al.*, 2018. Role of soil erosion in biogeochemical cycling of essential elements: carbon, nitrogen, and phosphorus. *The Annual Review of Earth and Planetary Sciences is Online at Earth.Annualreviews.Org*, 46, 521–569. doi:10.1146/annurev-earth-082517.
Birkinshaw, S.J., 2010. Technical note: automatic river network generation for a physically-based river catchment model. *Hydrology and Earth System Sciences*, 14 (9), 1767–1771.
Birkinshaw, S.J., 2021. SHETRAN standard version-V4.4.5 user guide and data input manual. Available from: https://research.ncl.ac.uk/shetran/
Birkinshaw, S.J. and Ewen, J., 2000. Modelling nitrate transport in the Slapton Wood catchment using SHETRAN. *Journal of Hydrology*, 230 (1-2), 18–33.
Bonsor, H.C., Macdonald, A.M., and Davies, J., 2014. Evidence for extreme variations in the permeability of laterite from a detailed analysis of well behaviour in Nigeria. *Hydrological Processes*, 28 (10), 3563–3573.
Bovolo, I., *et al.*, 2012. Fine-scale regional climate patterns in the Guianas, tropical South America, based on observations and reanalysis data. *International Journal of Climatology*, 32 (11), 1665–1689.
Bovolo, I., *et al.*, 2018. The Guiana Shield rainforests-overlooked guardians of South American climate. *Environmental Research Letters*, 13 (7), 1–2.
Bovolo, I., Parkin, G., and Wagner, T., 2009. Initial Assessment of the Climate of Guyana and the Region with a Focus on Iwokrama Main Report A 4 month pilot study supported by the Commonwealth Secretariat in collaboration with the Iwokrama International Centre for Rainforest Conservation and Development.
Buchhorn, M., *et al.*, 2020. Copernicus global land service: Land cover 100m: collection 3: epoch 2019: Globe.
Cucchi, M., *et al.*, 2020. WFDE5: Bias-adjusted ERA5 reanalysis data for impact studies. *Earth System Science Data*, 12 (3), 2097–2120.
Cucchi, M., *et al.*, 2022. *Near surface meteorological variables from 1979 to 2019 derived from bias-corrected reanalysis, version 2.1*. Copernicus Climate Change Service (C3S) Climate Data Store (CDS).
de Hipt, F.O., *et al.*, 2017. Applying SHETRAN in a tropical west African catchment (Dano, Burkina Faso)-calibration, validation, uncertainty assessment. *Water (Switzerland)*, 9 (2), 101.
Dembélé, M., *et al.*, 2020. Potential of satellite and reanalysis evaporation datasets for hydrological modelling under various model calibration strategies. *Advances in Water Resources*, 143, 103667.
Department of Environment, 2019. Green state development strategy.
de Souza, L.S., Armbruster, J.W., and Willink, P.W., 2020. Connectivity of neotropical river basins in the central Guiana Shield based on fish distributions. *Frontiers in Forests and Global Change*, 3 (8), 1–15.
Ebodé, V.B., 2022. Impact of rainfall variability and land-use changes on river discharge in Sanaga catchment (forest–savannah transition zone in Central Africa). *Hydrology Research*, 53 (7), 1017–1030.
Engman, E.T., 1986. Roughness coefficients for routing surface runoff. *Journal of Irrigation and Drainage Engineering*, 112, 39–53.
ESA, 2017. Land cover CCI product user. *Guide Version, 2.0*. Available from: maps.elie.ucl.ac.be/CCI/viewer/download/ESACCI-LC-Ph2-PUGv2_2.0.pdf
Ewen, J., Parkin, G., and O'Connell, P.E., 2000. Shetran: distributed river basin flow and transport modeling system. *ASCE Journal of Hydrologic Engineering*, 5, 250–258.
Getirana, A.C.V., *et al.*, 2012. The hydrological modeling and analysis platform (HyMAP): evaluation in the Amazon basin. *Journal of Hydrometeorology*, 13 (6), 1641–1665.
Giljum, S., *et al.*, 2022. A pantropical assessment of deforestation caused by industrial mining. *PNAS Sustainability Science*, 119 (38), 1–7.
Gleeson, T., *et al.*, 2014. A glimpse beneath earth's surface: GLobal HYdrogeology MaPS (GLHYMPS) of permeability and porosity. *Geophysical Research Letters*, 41 (11), 3891–3898.
GloH20, 2022. *MSWEP multi-source weighted-ensemble precipitation*. Available from: http://www.gloh2o.org/mswep/
Government of Guyana, 2016. *State of the environment report 2016*.
Gupta, H.V., *et al.*, 2009. Decomposition of the mean squared error and NSE performance criteria: implications for improving hydrological modelling. *Journal of Hydrology*, 377 (1–2), 80–91.
Gupta, H.V., Sorooshian, S., and Yapo, P.O., 1998. Toward improved calibration of hydrologic models: multiple and noncommensurable measures of information. *Water Resources Research*, 34 (4), 751–763.
Hartmann, J. and Moosdorf, N., 2012. The new global lithological map database GLiM: a representation of rock properties at the Earth surface. *Geochemistry, Geophysics, Geosystems*, 13 (12), 1–37.
Hassler, B. and Lauer, A., 2021. Comparison of reanalysis and observational precipitation datasets including ERA5 and WFDE5. *Atmosphere*, 12 (11), 1462.
Hersbach, H., *et al.*, 2020. The ERA5 global reanalysis. *Quarterly Journal of the Royal Meteorological Society*, 146 (730), 1999–2049.
Huang, T.H., *et al.*, 2012. Fluvial carbon fluxes in tropical rivers. *Current Opinion in Environmental Sustainability*, 4 (2), 162–169.
Huffman, G.J., *et al.*, 2018. NASA global precipitation measurement (GPM) integrated multi-satellitE retrievals for GPM (IMERG). Prepared for: Global Precipitation Measurement (GPM) National Aeronautics and Space Administration (NASA).
Huffman, G.J., *et al.*, 2020. Temperature and precipitation gridded data for global and regional domains derived from in-situ and satellite observations.
Huscroft, J., *et al.*, 2018. Compiling and mapping global permeability of the unconsolidated and consolidated earth: GLobal HYdrogeology

MaPS 2.0 (GLHYMPS 2.0). *Geophysical Research Letters*, 45 (4), 1897–1904.
HydroMet, 2009. *Daily flow data for Essequibo river at plantain Island*. Guyana: Ministry of Agriculture. Available from: http://hydromet.gov.gy/
Japan Aerospace Exploration Agency, 2021. ALOS world 3D 30 meter DEM. V3.2, January 2021.
Karra, K., *et al.*, 2021. Global land use/land cover with Sentinel 2 and deep learning. International Geoscience and Remote Sensing Symposium (IGARSS), 2021 July. 4704–4707.
Knoben, W.J.M., Freer, J.E., and Woods, R.A., 2019. Technical note: inherent benchmark or not? comparing Nash-Sutcliffe and Kling-Gupta efficiency scores. *Hydrology and Earth System Sciences*, 23 (10), 4323–4331.
Krysanova, V., *et al.*, 2020. How evaluation of global hydrological models can help to improve credibility of river discharge projections under climate change. *Climatic Change*, 163 (3), 1353–1377.
Lehner, B. and Grill, G., 2013. Global river hydrography and network routing: baseline data and new approaches to study the world's large river systems. *Hydrological Processes*, 27 (15), 2171–2186.
MacDonald, A.M., *et al.*, 2012. Quantitative maps of groundwater resources in Africa. *Environmental Research Letters*, 7 (024009), 1–7.
Meybeck, M. and Ragu, A., 2012. GEMS-GLORI world river discharge database. *PANGAEA*.
Mohan, M.M.P., Kanchirapuzha, R., and Varma, M.R.R., 2020. Review of approaches for the estimation of sensible heat flux in remote sensing-based evapotranspiration models. *Journal of Applied Remote Sensing*, 14 (4), 1–31.
Montzka, C., *et al.*, 2017. A global data set of soil hydraulic properties and sub-grid variability of soil water retention and hydraulic conductivity curves. *Earth System Science Data*, 9 (2), 529–543.
Moriasi, D.N., *et al.*, 2015. Hydrologic and water quality models: performance measures and evaluation criteria. *Transactions of the ASABE*, 58 (6), 1763–1785.
Muñoz-Sabater, J., *et al.*, 2021. ERA5-Land: a state-of-the-art global reanalysis dataset for land applications. *Earth System Science Data*, 13 (9), 4349–4383.
Muñoz Sabater, J., 2019. *ERA5-Land hourly data from 1981 to present*. Copernicus Climate Change Service (C3S) Climate Data Store (CDS).
Nkiaka, E., *et al.*, 2022. Evaluating the accuracy of gridded water resources reanalysis and evapotranspiration products for assessing water security in poorly gauged basins. *Hydrology and Earth System Sciences*, 26 (22), 5899–5916.
OpenStreetMap, 2017. *Planet dump*. Available from: https://planet.osm.org.https://www.openstreetmap.org
Parkin, G., *et al.*, 1996. Validation of catchment models for predicting land-use and climate change impacts. 2. Case study for a Mediterranean catchment. *Journal of Hydrology*, 175, 595–613.
Pendrill, F., *et al.*, 2022. Disentangling the numbers behind agriculture-driven tropical deforestation. *Science*, 377 (6611), 1–11.
Pereira, R., *et al.*, 2014a. Seasonal patterns of rainfall and river isotopic chemistry in northern Amazonia (Guyana): from the headwater to the regional scale. *Journal of South American Earth Sciences*, 52, 108–118.
Pereira, R., *et al.*, 2014b. Mobilization of optically invisible dissolved organic matter in response to rainstorm events in a tropical forest headwater river. *Geophysical Research Letters*, 41 (4), 1202–1208.
Raymond, P.A. and Spencer, R.G.M., 2015. Riverine DOM. In: D.A. Hansell and C.A. Carlson, eds. *Biogeochemistry of marine dissolved organic matter*, 2nd ed. Elsevier Inc, 509–533.
Regnier, P., *et al.*, 2013. Anthropogenic perturbation of the carbon fluxes from land to ocean. *Nature Geoscience*, 6 (8), 597–607.
Saatchi, S.S., *et al.*, 2011. Benchmark map of forest carbon stocks in tropical regions across three continents. *Proceedings of the National Academy of Sciences of the United States of America*, 108 (24), 9899–9904.
Satgé, F., *et al.*, 2021. Are gridded precipitation datasets a good option for streamflow simulation across the Juruá river basin Amazon? *Journal of Hydrology*, 602, 1–16.
Schneider, K.E. and Hogue, T.S., 2022. Calibration of a hydrologic model in data-scarce Alaska using satellite and other gridded products. *Journal of Hydrology: Regional Studies*, 39, 100979.
Senay, G.B., Kagone, S., and Velpuri, N.M., 2020. Operational global actual evapotranspiration: development, evaluation, and dissemination. *Sensors (Switzerland)*, 20 (7), 1915.
Shangguan, W., *et al.*, 2017. Mapping the global depth to bedrock for land surface modeling. *Journal of Advances in Modeling Earth Systems*, 9 (1), 65–88.
Sheffield, J., *et al.*, 2018. Satellite remote sensing for water resources management: potential for supporting sustainable development in data-poor regions. *Water Resources Research*, 54 (12), 9724–9758.
Sreedevi, S., *et al.*, 2019. Multiobjective sensitivity analysis and model parameterization approach for coupled streamflow and groundwater table depth simulations using SHETRAN in a wet humid tropical catchment. *Journal of Hydrology*, 579, 1–20.
Sreedevi, S. and Eldho, T.I., 2021. Effects of grid-size on effective parameters and model performance of SHETRAN for estimation of streamflow and sediment yield. *International Journal of River Basin Management*, 19 (4), 535–551.
Stacke, T. and Hagemann, S., 2021. Hydropy (v1.0): a new global hydrology model written in Python. *Geoscientific Model Development*, 14 (12), 7795–7816.
Sun, Q., *et al.*, 2018. A review of global precipitation data sets: data sources, estimation, and intercomparisons. *Reviews of Geophysics*, 56 (1), 79–107.
Telteu, C.E., *et al.*, 2021. Understanding each other's models: an introduction and a standard representation of 16 global water models to support intercomparison, improvement, and communication. *Geoscientific Model Development*, 14 (6), 3843–3878.
Towner, J., *et al.*, 2019. Assessing the performance of global hydrological models for capturing peak river flows in the Amazon basin. *Hydrology and Earth System Sciences*, 23 (7), 3057–3080.
US Army Corps of Engineers, 1998. *Water resources assessment of Guyana*.
Wang, C., *et al.*, 2022. Evaluation of three gridded potential evapotranspiration datasets for streamflow simulation in three inland river basins in the arid Hexi Corridor, Northwest China. *Journal of Hydrology: Regional Studies*, 44, 1–17.
Ward, P.J., *et al.*, 2014. Annual flood sensitivities to El Niño–Southern Oscillation at the global scale. *Hydrology and Earth System Sciences*, 18 (1), 47–66.
Wieder, W., *et al.*, 2014. *Regridded harmonized world soil database v1.2*. ORNL Distributed Active Archive Center.
Wongchuig, S.C., *et al.*, 2019. Hydrological reanalysis across the 20th century: a case study of the Amazon basin. *Journal of Hydrology*, 570, 755–773.
Wu, J., *et al.*, 2020. The reliability of global remote sensing evapotranspiration products over Amazon. *Remote Sensing*, 12 (14), 1–19.
WWF, 2020. World wildlife fund project: eco-hydrological assessment of the North Rupununi Wetlands: monitoring and assessment.
Yamazaki, D., *et al.*, 2017. A high-accuracy map of global terrain elevations. *Geophysical Research Letters*, 44 (11), 5844–5853.
Yang, W., *et al.*, 2022. The impact of calibration conditions on the transferability of conceptual hydrological models under stationary and nonstationary climatic conditions. *Journal of Hydrology*, 613, 1–11.
Zhu, W., *et al.*, 2022. Multi-scale evaluation of global evapotranspiration products derived from remote sensing images: accuracy and uncertainty. *Journal of Hydrology*, 611, 1–20.